On the symmetry of the impedance matrix for acoustic radiation modes and sound power evaluation

H. Peters (1), S. Marburg (2) and N. Kessissoglou (1)

(1) School of Mechanical and Manufacturing Engineering, The University of New South Wales, Sydney, NSW 2052, Australia
(2) LRT4 – Institute of Mechanics, Universität der Bundeswehr München, D-85579 Neubiberg, Germany

ABSTRACT

By identifying the efficiently radiating acoustic radiation modes of a fluid loaded vibrating structure, the storage requirements of the acoustic impedance matrix for calculation of the sound power using the boundary element method can be greatly reduced. In order to compute the acoustic radiation modes, the impedance matrix needs to be symmetric. However, when using the boundary element method, it is often found that the impedance matrix is not symmetric. This paper describes the origin of the asymmetry of the impedance matrix and presents a simple way to generate symmetry. The introduction of additional errors when symmetrising the impedance matrix must be avoided. An example is used to demonstrate the behaviour of the asymmetry and the effect of symmetrization of the impedance matrix on the sound power. The application of the technique presented in this work to compute the radiated sound power of a submerged marine vessel is discussed.

INTRODUCTION

Acoustic radiation modes have become a popular tool for sound power computation and acoustic characterization of structures in exterior acoustics since its introduction in 1990 (Borgiotti, 1990). Acoustic radiation modes are the eigenvectors of the acoustic impedance matrix and form an orthogonal set of linearly independent surface velocity distributions. Since the acoustic radiation modes diagonalize the impedance matrix, the total radiated sound power is the sum of all independently radiating sound power contributions of each mode. Additionally, the eigenvalue associated with each acoustic radiation mode is proportional to the radiation efficiency of each modal contribution. An important property of acoustic radiation modes is that at low frequencies, a very small number of the most efficiently radiating acoustic radiation modes dominate the sound radiation in to the far field (Elliott and Johnson, 1993). For example, Naghshineh et al. (1992, 1998) exploited the use of the efficiently radiating acoustic modes to minimise sound power radiated from a beam and a cylindrical shell with end caps using an active control strategy.

Reciprocity relations have been used to show that the acoustic impedance matrix must be symmetric (Chen and Ginsberg, 1995). The reciprocity relation states that an interchange of a sender and a receiver in an acoustic field will not affect the receiver signal. Many other researchers confirm the symmetry of the impedance matrix in the context of radiated sound power (Borgiotti, 1990; Cunefare, 1991; Cunefare and Currey, 1994; Cunefare et al., 2001). Cunefare et al. (2001) appear to be the first to comment on deviations from symmetry of the impedance matrix. They noticed that in the boundary element method, the impedance matrix is not symmetric. They attribute this asymmetry to differences in element area associated with each node in the discretised model. It will be shown in this article that this is not the reason for the asymmetry of the impedance matrix.

The aim of this paper is to examine the cause and extent of the asymmetry of the acoustic impedance matrix. It is shown that the observed asymmetry of the acoustic impedance matrix is due to a discretization error that is inevitable when discretizing the symmetric impedance operator using collocation BEM (Cunefare et al., 2001). An h-convergence study shows that the error decreases with a constant rate of convergence. It is also shown that the effect of asymmetry on an acoustic radiation mode decreases with increasing radiation efficiency of that mode. Finally, it is demonstrated that computing the symmetric part of the acoustic impedance matrix provides a simple tool for symmetrization of the acoustic impedance matrix, without introducing any significant errors with respect to calculation of the sound power using a truncated series of acoustic radiation modes.

RADIATED SOUND POWER

In time-harmonic and linear acoustics, the total radiated sound power P is defined as

$$P = \frac{1}{2}\Re\left\{\int_\Gamma p(\mathbf{x})v^*(\mathbf{x})\,\mathrm{d}\Gamma(\mathbf{x})\right\} \tag{1}$$

where p is sound pressure, v is velocity, Γ is the boundary circumscribing the radiating object and $(\cdot)^*$ denotes the conjugate complex. The goal is to compute the acoustic radiation modes with respect to velocity. The formulation of the quadratic eigenvalue problem requires rearranging Eq. (1) as an expression that is quadratic in velocity v. Thus a relationship of the form

$$\mathscr{L}_p\left(p(\mathbf{x})\right) = \mathscr{L}_v\left(v(\mathbf{x})\right) \tag{2}$$

is required (Chen and Ginsberg, 1995). $\mathscr{L}_p$ and $\mathscr{L}_v$ are linear operators with respect to p and v. Solving Eq. (2) for sound pressure p and substitution into Eq. (1) yields

$$P = \frac{1}{2}\Re\left\{\int_\Gamma \mathscr{L}_p^{-1}\mathscr{L}_v\left(v(\mathbf{x})\right)v^*(\mathbf{x})\,\mathrm{d}\Gamma(\mathbf{x})\right\}. \tag{3}$$

To enable an algebraic treatment of the quadratic eigenvalue problem, Eqs. (1) and (2) are discretised. Using N basis functions $\phi_l(\mathbf{x})$, the continuous variables p and v are approximated by (Marburg and Nolte, 2008)

$$p(\mathbf{x}) = \sum_{l=1}^{N}\phi_l(\mathbf{x})\mathbf{p} = \phi^T(\mathbf{x})\mathbf{p}\,, \qquad v(\mathbf{x}) = \sum_{l=1}^{N}\phi_l(\mathbf{x})\mathbf{v} = \phi^T(\mathbf{x})\mathbf{v}. \tag{4}$$

Substitution of Eq. (4) into Eq. (1) yields

$$P = \frac{1}{2}\Re\left\{\mathbf{p}^T\Theta\mathbf{v}^*\right\} \tag{5}$$

where $\mathbf{\Theta}$ is the boundary mass matrix and is given by

$$\mathbf{\Theta} = \int_{\Gamma} \phi(\mathbf{x})\phi^T(\mathbf{x})\,\mathrm{d}\Gamma(\mathbf{x}). \tag{6}$$

Eq. (5) is the result of discretisation of Eq. (1). Application of the boundary element method and discretization by collocation (collocation BEM) to Eq. (2) leads to the following matrix equation (Marburg and Nolte, 2008)

$$\mathbf{Hp} = \mathbf{Gv}. \tag{7}$$

Solving Eq. (7) for sound pressure $\mathbf{p}$ and substitution into the discretised expression for sound power in Eq. (5) yields a discretised expression for sound power that is a quadratic in terms of velocity $\mathbf{v}$

$$P = \frac{1}{2}\Re\left\{\mathbf{v}^T\left(\mathbf{H}^{-1}\mathbf{G}\right)^T\mathbf{\Theta}\mathbf{v}^*\right\} = \frac{1}{2}\Re\left\{\mathbf{v}^T\mathbf{Z}\mathbf{v}^*\right\}. \tag{8}$$

$\mathbf{Z} = \left(\mathbf{H}^{-1}\mathbf{G}\right)^T\mathbf{\Theta}$ is the acoustic impedance matrix. It is important to note that theoretically, $\mathbf{Z}$ should be a symmetric matrix (Chen and Ginsberg, 1995). However, due to the discretisation error in collocation BEM, $\mathbf{Z}$ is no longer a symmetric matrix (Cunefare et al., 2001).

RADIATION EFFICIENCY AND ACOUSTIC RADIATION MODES

The radiation efficiency σ is defined as the ratio of the sound power P from Eq. (8) and the reference sound power $\bar{P}$ from the same object radiating with the spatial mean velocity $\bar{v} = |v(\mathbf{x})|$. The reference sound power $\bar{P}$ is given by

$$\bar{P} = \frac{1}{2}\Re\left\{\int_{\Gamma}\overline{pv^*}\,\mathrm{d}\Gamma(\mathbf{x})\right\} \tag{9}$$

and using the specific acoustic impedance $z = \rho_0 c$, the radiation efficiency becomes

$$\sigma = \frac{P}{\bar{P}} = \frac{P}{\frac{\rho_0 c}{2}\int_{\Gamma}|v(\mathbf{x})|^2\,\mathrm{d}\Gamma(\mathbf{x})}. \tag{10}$$

Discretisation of Eq. (10) is performed in a similar way to the discretisation of Eq. (1) and yields

$$\sigma = \frac{1}{\rho_0 c}\frac{\Re\left\{\mathbf{v}^T\mathbf{Z}\mathbf{v}^*\right\}}{\mathbf{v}^T\mathbf{\Theta}\mathbf{v}^*}. \tag{11}$$

For symmetric $\mathbf{Z}$, the expression for the radiated sound power in Eq. (8) can be simplified to

$$P = \frac{1}{2}\Re\left\{\mathbf{v}^T\mathbf{Z}\mathbf{v}^*\right\} = \frac{1}{2}\mathbf{v}^T\Re\left\{\mathbf{Z}\right\}\mathbf{v}^* = \frac{1}{2}\mathbf{v}^T\mathbf{Z}_R\mathbf{v}^* \tag{12}$$

where $\mathbf{Z}_R$ is the resistive part of the acoustic impedance matrix resulting in real radiated sound power (Chen and Ginsberg, 1995). From hereafter, $\mathbf{Z}_R$ is referred to as the acoustic resistance matrix. Mathematically speaking, the simplification in Eq. (12) is only applicable for symmetric $\mathbf{Z}$, however here it will also be used for asymmetric $\mathbf{Z}$. It is shown that the effect of the asymmetry of $\mathbf{Z}$ on computed results such as sound power and radiation efficiency is small. Hence, irrespective of the symmetry properties of $\mathbf{Z}$, the radiation efficiency in Eq. (11) is rewritten as

$$\sigma = \frac{1}{\rho_0 c}\frac{\mathbf{v}^T\mathbf{Z}_R\mathbf{v}^*}{\mathbf{v}^T\mathbf{\Theta}\mathbf{v}^*}. \tag{13}$$

Eq. (13) leads to the generalised eigenvalue problem and, for an asymmetric $\mathbf{Z}_R$, right and left eigenvectors are computed which are respectively given by

$$\mathbf{Z}_R\psi_r = \lambda\mathbf{\Theta}\psi_r\,, \qquad \mathbf{Z}_R^T\psi_l = \lambda\mathbf{\Theta}^T\psi_l. \tag{14}$$

The radiation efficiency σ is related to the eigenvalue λ by $\lambda = \rho_0 c\sigma$. The eigenvectors ψ_r and ψ_r form the right and left modal matrices ψ_r and ψ_l, respectively. It is important to note that for asymmetric $\mathbf{Z}_R$, the eigenvectors are complex and nonphysical (Cunefare et al., 2001) and hence can not be called acoustic radiation modes. The eigenvectors are normalised so that (Zurmühl and Falk, 1997)

$$\psi_l^T\mathbf{\Theta}\psi_r = \mathbf{I}\,, \qquad \psi_l^T\mathbf{Z}_R\psi_r = \mathbf{\Lambda} \tag{15}$$

where $\mathbf{I}$ is the identity matrix and $\mathbf{\Lambda} = \mathrm{diag}\left\{\lambda_j\right\}$. If the acoustic resistance matrix $\mathbf{Z_R}$ is symmetric, the eigenvectors of $\mathbf{Z}_R$ become $\psi = \psi_r = \psi_l$ and are real values. In this case, the eigenvectors are equivalent to the well-known acoustic radiation modes. The acoustic radiation modes form a set of orthogonal basis functions. Choosing an appropriate set of modal participation coefficients $\boldsymbol{\zeta}$, the superposition of these basis functions allows the reproduction of an arbitrary surface velocity pattern via

$$\mathbf{v} = \psi\boldsymbol{\zeta}. \tag{16}$$

Left multiplication of Eq. (16) with $\psi^T\mathbf{\Theta}$ and consideration of Eq. (15) yields the modal participation coefficients

$$\boldsymbol{\zeta} = \psi^T\mathbf{\Theta}\mathbf{v}. \tag{17}$$

Based on Eq. (8) and under consideration of Eqs. (12), (16), (15) and a *symmetric* $\mathbf{Z}_R$, the radiated sound power can be recovered from the normalised eigenvalues and eigenvectors via

$$P_{sym} = \frac{1}{2}\boldsymbol{\zeta}^T\mathbf{\Lambda}\boldsymbol{\zeta}^* = \frac{1}{2}\mathbf{v}^T\mathbf{\Theta}\psi\mathbf{\Lambda}\psi^T\mathbf{\Theta}\mathbf{v}^*. \tag{18}$$

Eq. (18) also holds when using a reduced number of radiation modes ψ_k.

MEASURES OF ASYMMETRY AND SYMMETRISATION

Measures of Asymmetry

In order to assess the degree of asymmetry, three measures are defined. They are discussed in what follows.

Modal Assurance Criterion

The Modal Assurance Criterion (MAC) provides an indication of the correlation between two vectors (modes) $\mathbf{a}$ and $\mathbf{b}$ via (Allemang, 2002)

$$\mathrm{MAC}(\mathbf{a},\mathbf{b}) = \frac{\left|\mathbf{a}^H\mathbf{b}\right|^2}{\left(\mathbf{a}^H\mathbf{a}\right)\left(\mathbf{b}^H\mathbf{b}\right)} \tag{19}$$

If $\mathbf{Z}_R$ is symmetric, MAC(ψ_r, ψ_l) is equal to unity for all eigenvectors of $\mathbf{Z}_R$. For asymmetric $\mathbf{Z}_R$, the MAC values are between zero and one.

Mean Deviation from Symmetry

In the matrix $\mathbf{Z}_R$, the symmetry error ε_{kl} of the matrix entry $z_{R,kl}$ is defined as

$$\varepsilon_{kl} = 2\left|\frac{z_{R,lk} - z_{R,kl}}{z_{R,lk} + z_{R,kl}}\right| \tag{20}$$

The mean deviation from symmetry is then defined as the mean value of all ε_{kl}

$$\varepsilon = \frac{1}{N^2}\sum_{k=1}^{N}\sum_{l=1}^{N}\varepsilon_{kl} \tag{21}$$

A symmetric matrix $\mathbf{Z}_R$ results in $\varepsilon = 0$. Increasing values of ε indicate an increasing deviation from symmetry.

Asymmetric Fill of $\mathbf{Z}_R$

A pair of matrix entries $z_{R,kl}$ and $z_{R,lk}$ is considered symmetric if

$$z_{R,lk} - z_{R,kl} < \tau \frac{z_{R,lk} + z_{R,kl}}{2} \tag{22}$$

where τ is the threshold for symmetry. The share of asymmetric $z_{R,kl}$ and $z_{R,lk}$ of the N^2 matrix entries of $\mathbf{Z}_R$ is termed asymmetric fill κ of $\mathbf{Z}_R$. Again, $\kappa = 0$ indicates a symmetric matrix $\mathbf{Z}_R$.

Symmetrisation of $\mathbf{Z}_R$

Symmetrisation of $\mathbf{Z}_R$ is simply achieved by calculating the symmetric part of $\mathbf{Z}_R$ (Weisstein).

$$\mathbf{Z}_{R,sym} = \frac{\mathbf{Z}_R^T + \mathbf{Z}_R}{2} \tag{23}$$

Other methods for symmetrisation are available but will not be used in this study. For example, $\mathbf{Z}_R$ can also be symmetrised by taking the strictly upper triangular matrix $\mathbf{U}$ and the main diagonal $\mathbf{D}$ of $\mathbf{Z}_R$ and computing $\mathbf{Z}_{R,sym2} = \mathbf{U}^T + \mathbf{U} + \mathbf{D}$.

MODEL

A simplified model of the pressure hull of a submarine (Fig. 1) is investigated. The cylindrical section is 45 m long with a 6.5 m diameter. The acoustic fluid is water with density $\rho = 1000\,\mathrm{kg/m^3}$ and speed of sound $c_0 = 1482\,\mathrm{m/s}$. The acoustic fluid is modelled using 4-node super-parametric discontinuous linear boundary elements in AKUSTA, a non-commercial code developed by the author Marburg and co-workers (Marburg and Schneider, 2003; Marburg and Amini, 2005). Fig. 1 illustrates that discontinuous boundary elements do not have to match at their edges. The cylinder in Fig. 1 is shown with the coarsest discretisation used in this study (seed = 1). Table 1 lists the different mesh seeds and the corresponding number of elements.

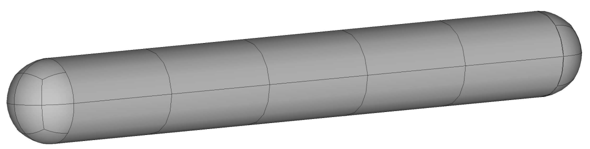

Figure 1: Cylinder with hemispherical end caps

Table 1: Mesh seeds d, maximum element size h and corresponding degrees of freedom (DOF)

d	h (m)	DOF
1	9	176
2	4.5	704
4	2.25	2816
8	1.125	11264

RESULTS

H-Convergence

The results of the h-convergence study for the cylinder are presented. Figs. 2 and 3 show the mean error ε and the asymmetric fill κ versus seed d at 10 Hz and 100 Hz. The threshold for symmetry τ is not equal for calculations at 10 Hz and at 100 Hz. This difference is due to the fact that for calculations at 10 and 100 Hz, the same discretisations are used despite the one order of magnitude difference in wavelength in the acoustic fluid.

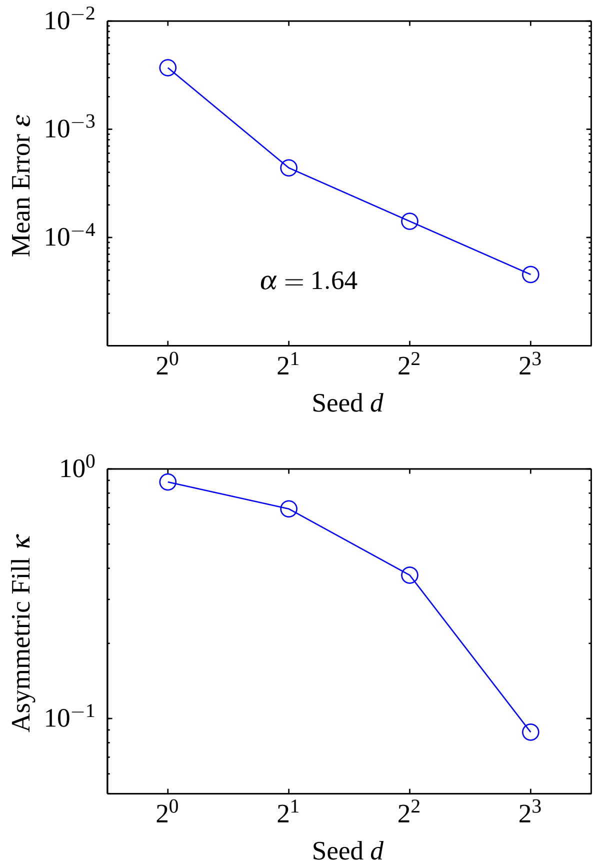

Figure 2: Mean error and asymmetric fill ($\tau = 10^{-4}$) for the cylinder at 10 Hz

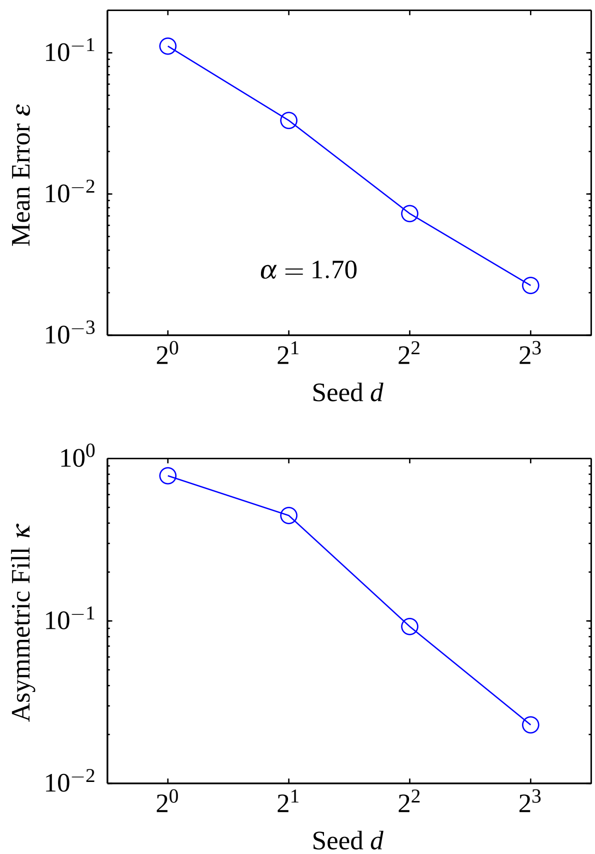

Figure 3: Mean error and asymmetric fill ($\tau = 10^{-2}$) for the cylinder at 100 Hz

This choice is made because of the prohibitive cost of models with more than 12000 degrees of freedom. It is found that the error dependence is of the form

$$\varepsilon(d,k) \sim C(k)d^{-\alpha} \tag{24}$$

where k is the wave number, $C(k)$ is a constant with respect to mesh seed d and α is the rate of convergence. A similar relationship applies to the asymmetric fill κ versus seed d. Figs. 2 and 3 show that the measures of asymmetry decrease with a constant rate of convergence α. This demonstrates that a discretisation error introduced by the approximations in Eq. (4) is responsible for the asymmetry of the acoustic impedance matrix $\mathbf{Z}$.

MAC

Figs. 4 and 5 present the modal assurance criterion and the radiation efficiency for the coarsest and finest discretisation at 100 Hz for the cylinder model. Correlation of the right ψ_r and left ψ_l eigenvectors can be observed in Fig. 4. The MAC(ψ_r, ψ_l) values demonstrate that the eigenvectors correlate very well for low mode numbers which correspond to high and medium radiation efficiencies σ. Examination of the results for the cylinder model with 11264 degrees of freedom shows that once the initial decay of the radiation efficiency has stopped at about $\sigma \approx 10^{-5}$, the MAC value decreases rapidly and almost no correlation between the right and left eigenvectors remains, especially at high frequencies. The transition from a good correlation to a poor correlation of eigenvectors occurs rapidly. The eigenvectors that correspond to a radiation efficiency of $\sigma > 10^{-5}$ are hardly affected by the asymmetry of the acoustic resistance matrix $\mathbf{Z}_R$. Even for boundary element models with much fewer elements, this effect is clearly visible. Furthermore, the transition point at which the correlation of the right and left eigenvectors switches from good to poor is still $\sigma \approx 10^{-5}$. The next question that arises is how the eigenvectors ψ_r or ψ_l using an asymmetric $\mathbf{Z}_R$ correlate with the acoustic radiation modes ψ using a symmetric $\mathbf{Z}_{R,sym}$. Fig. 5 shows the MAC(ψ_r, ψ) values and compares them to the corresponding radiation efficiencies. Similar to previous observations, it is found that the efficiently radiating acoustic radiation modes correlate very well with the right eigenvectors obtained from the eigenvalue problem with asymmetric $\mathbf{Z}_R$. The transition between good and poor correlation is even more abrupt but the critical radiation efficiency $\sigma \approx 10^{-5}$ still holds. MAC(ψ_l, ψ) is not shown because MAC(ψ_r, ψ) and MAC(ψ_l, ψ) yield virtually indistinguishable results. It is concluded that efficiently radiating acoustic radiation modes are hardly affected by an asymmetry of the acoustic resistance matrix $\mathbf{Z}_R$. The asymmetry of $\mathbf{Z}_R$ seems to only be reflected in the eigenvectors that correspond to low radiation efficiencies of $\sigma < 10^{-5}$.

Radiated Sound Power

For comparison, the radiated sound power is calculated using five different expressions. The reference value P_{ref} is obtained from Eq. (8). A second (P) and third (P_{sym}) value for the radiated sound power are obtained from Eqs. (12) and (18), respectively. Note that Eqs. (8) and (12) are not equal for asymmetric $\mathbf{Z}_R$ since the simplification that leads to Eq. (12) is only valid for symmetric $\mathbf{Z}_R$. In contrast to these equations, Eq. (18) is based on the symmetrised $\mathbf{Z}_{R,sym}$. Similarly to Eq. (18), the radiated sound power may also be recovered from $\mathbf{\Lambda}$, ψ_r and ψ_l, which are obtained from the asymmetric $\mathbf{Z}_R$ via

$$P_r = \frac{1}{2}\zeta_r^T \mathbf{\Lambda} \zeta_r^* \tag{25}$$

$$P_l = \frac{1}{2}\zeta_l^T \mathbf{\Lambda} \zeta_l^* . \tag{26}$$

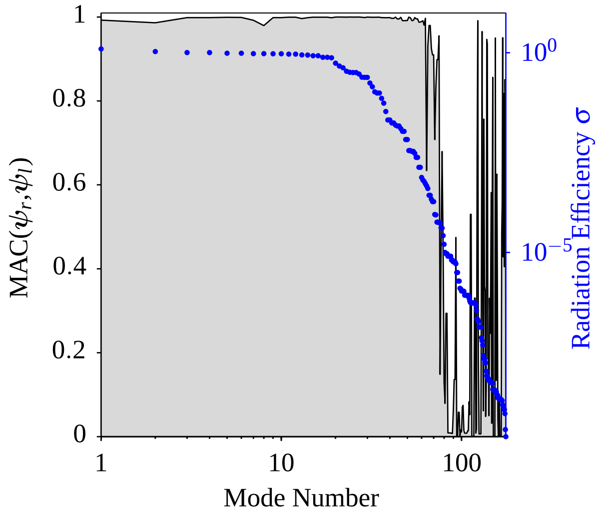

(a) 176 degrees of freedom

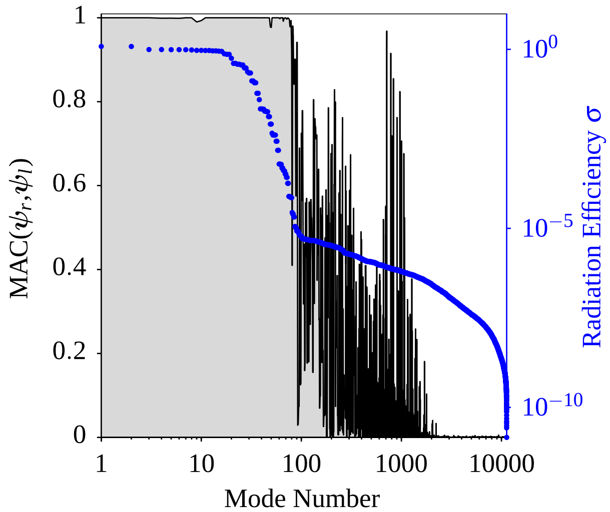

(b) 11264 degrees of freedom

Figure 4: MAC(ψ_r, ψ_l) and σ for the cylinder model at 100 Hz

Note that Eqs. (25) and (26) are physically questionable and are used here solely for the purpose of comparison.

Figs. 6 and 7 show the real and imaginary parts of P, P_{sym}, P_r and P_l normalised by the real reference value P_{ref}. The velocity $\mathbf{v}$ is a random and complex $N \times 1$ vector. The real part of P according to Eq. (12) is not affected by the simplification which is strictly speaking not valid for asymmetric $\mathbf{Z}_R$. This simplification does, however, create a non-physical imaginary part of P which decreases with increasing discretisation. As a result, it is found that $P_{ref} = \Re\{P\}$ even for asymmetric $\mathbf{Z}_R$. The value of P_{sym} according to Eq. (18) using the symmetrised $\mathbf{Z}_R$ is identical to P_{ref}, thus $P_{ref} = P_{sym}$. It can therefore be concluded that symmetrisation of $\mathbf{Z}_R$ has no effect on the accuracy of the radiated sound power. The real part of the values of P_r and P_l deviates significantly from P_{ref} at coarse discretisations but converges to the reference value with increasing degrees of freedom. The deviation of the imaginary parts of P_r and P_l are close to zero for all discretisations. This illustrates that as the discretisation error decreases, the eigenvectors ψ_r and ψ_l converge towards the acoustic radiation modes ψ.

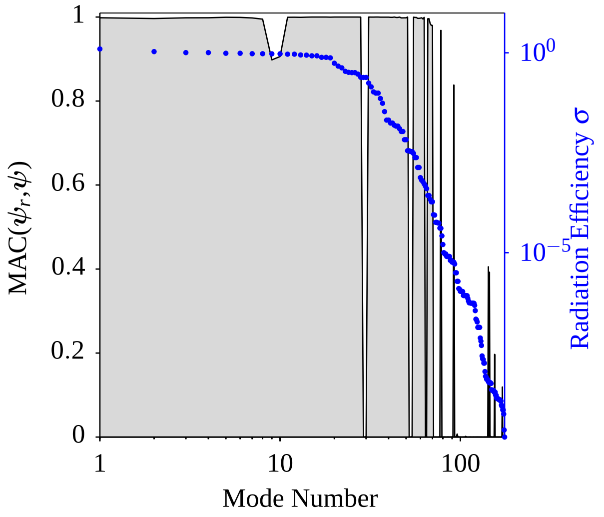

(a) 176 degrees of freedom

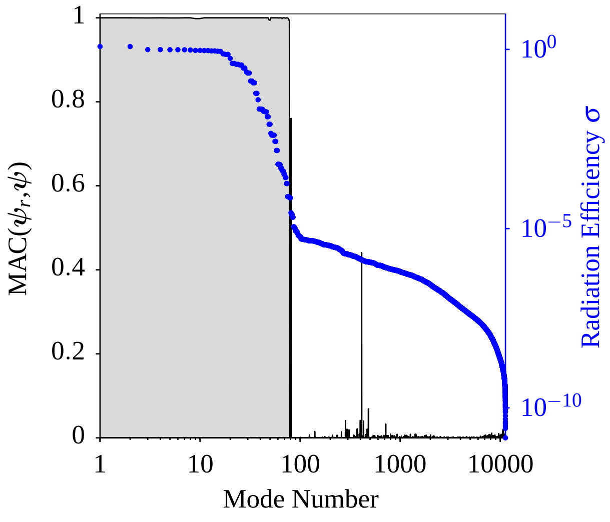

(b) 11264 degrees of freedom

Figure 5: MAC(ψ_r,ψ) and σ for the cylinder model at 100 Hz

CONCLUSIONS

In this paper, the asymmetry of the acoustic impedance matrix $\mathbf{Z}$ has been investigated. It was demonstrated that the symmetry error decreases with increasing degrees of freedom of the computational model. This shows that the discretisation error is the major source for the observed asymmetry of $\mathbf{Z}$ using collocation BEM. It is further demonstrated that simply taking the symmetric part of the acoustic resistance matrix $\mathbf{Z}_R$ supplies an adequate and convenient way of symmetrising $\mathbf{Z}_R$ without introducing any additional errors with respect to the radiated sound power and the acoustic radiation modes. Justified by the acoustic reciprocity theorem and the conclusion that the impedance relationship must be symmetric (Chen and Ginsberg, 1995), even a numerical method such as the collocation BEM that yields an asymmetric impedance matrix is perfectly suitable for the analysis of acoustic radiation modes.

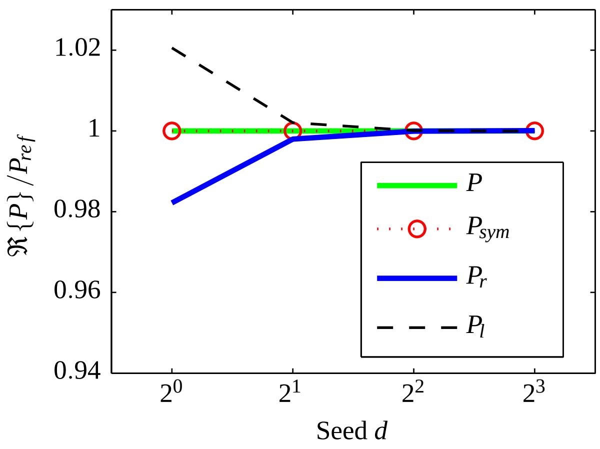

Figure 6: Sound power comparison for the cylinder model at 100 Hz (real part)

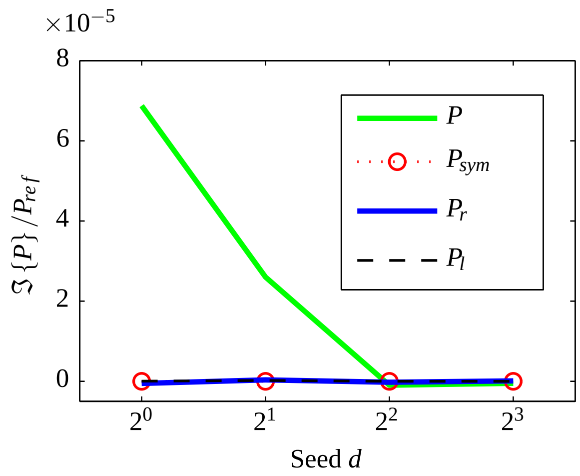

Figure 7: Sound power comparison for the cylinder model at 100 Hz (imaginary part)

REFERENCES

Allemang, RJ (2002). "The Modal Assurance Criterion (MAC): twenty years of use and abuse". *Proceedings of the 20th International Modal Analysis Conference*. Los Angeles, CA, USA.

Borgiotti, GV (1990). "The power radiated by a vibrating body in an acoustic fuid and its determination from boundary measurements". *Journal of the Acoustical Society of America* 88, pp. 1884–1893.

Chen, PT and Ginsberg, JH (1995). "Complex power, reciprocity, and radiation modes for submerged bodies". *Journal of the Acoustical Society of America* 98, pp. 3343–3351.

Cunefare, KA (1991). "The minimum multimodal radiation efficiency of baffled finite beams". *Journal of the Acoustical Society of America* 90, pp. 2521–2529.

Cunefare, KA and Currey, MN (1994). "On the exterior acoustic radiation modes of structures". *Journal of the Acoustical Society of America* 96, pp. 2302–2312.

Cunefare, KA, Currey, MN, Johnson, ME, and Elliot, SJ (2001). "The radiation efficiency grouping of free-space acoustic radiation modes". *Journal of the Acoustical Society of America* 109, pp. 203–215.

Elliott, SJ and Johnson, ME (1993). "Radiation modes and the active control of sound power". *Journal of the Acoustical Society of America* 94, pp. 2194–2204.

Marburg, S and Amini, S (2005). "Cat's eye radiation with boundary elements: comparative study on treatment of irregular frequencies". *Journal of Computational Acoustics* 13, pp. 21–45.

Marburg, S and Nolte, B, eds. (2008). *Computational acoustics of noise propagation in fluids*. Berlin: Springer.

Marburg, S and Schneider, S (2003). “Influence of element types on numeric error for acoustic boundary elements”. *Journal of Computational Acoustics* 11, pp. 363–386.

Naghshineh, K and Koopmann, GH (1992). “A design method for achieving weak radiator structures using active vibration control”. *Journal of the Acoustical Society of America* 92, pp. 856–870.

Naghshineh, K, Chen, W, and Koopmann, GH (1998). “Use of acoustic basis functions for active control of sound power radiated from a cylindrical shell”. *Journal of the Acoustical Society of America* 103, pp. 1897–1903.

Weisstein, EW. *Symmetric part*. From *MathWorld*–A Wolfram Web Resource. `http://mathworld.wolfram.com/SymmetricPart.html`. Accessed online on 26/08/2011.

Zurmühl, R and Falk, S (1997). *Matrizen 1*. Berlin: Springer.